A&A 605, C4 (2017)
DOI: 10.1051/0004-6361/201322953e

Astronomy & Astrophysics

Hot horizontal branch stars in NGC 288 – effects of diffusion and stratification on their atmospheric parameters *(Corrigendum)*

S. Moehler[1,2], S. Dreizler[3], F. LeBlanc[4], V. Khalack[4], G. Michaud[5], J. Richer[5], A. V. Sweigart[6], and F. Grundahl[7]

[1] European Southern Observatory, Karl-Schwarzschild-Str. 2, 85748 Garching, Germany
e-mail: smoehler@eso.org
[2] Institut für Theoretische Physik und Astrophysik, Olshausenstraße 40, 24118 Kiel, Germany
[3] Georg-August-Universität, Institut für Astrophysik, Friedrich-Hund-Platz 1, 37077 Göttingen, Germany
[4] Département de Physique et d'Astronomie, Université de Moncton, Moncton, New Brunswick, E1A 3E9, Canada
[5] Département de physique, Université de Montréal, Montréal, Québec, H3C 3J7, Canada
[6] NASA Goddard Space Flight Center, Exploration of the Universe Division, Code 667, Greenbelt, MD 20771, USA
[7] Stellar Astrophysics Centre, Department of Physics & Astronomy, University of Århus, Ny Munkegade 120, 8000 Århus C, Denmark

A&A 565, A100 (2014), DOI: 10.1051/0004-6361/201322953
This corrigendum also includes modifications to:
A&A 526, A136 (2011), DOI: 10.1051/0004-6361/201015020
A&A 474, 505 (2007), DOI: 10.1051/0004-6361:20078184
A&A 455, 943 (2006), DOI: 10.1051/0004-6361:20065427
A&A 414, 181 (2004), DOI: 10.1051/0004-6361:20031606
A&A 405, 135 (2003), DOI: 10.1051/0004-6361:20030622
A&A 383, 938 (2002), DOI: 10.1051/0004-6361:20020127
A&A 361, 937 (2000)
A&A 360, 120 (2000)
A&A 340, 305 (1998)
A&A 335, 510 (1998)
A&A 327, 577 (1997)
A&A 319, 109 (1997)
A&A 294, 65 (1995)
A&A 292, 261 (1994)
A&A 287, 38 (1994)
A&A 286, 925 (1994)
A&A 273, 524 (1993)
A&A 239, 265 (1990)
MNRAS 370, 151 (2006)
MNRAS 352, 1279 (2004)

ABSTRACT

We found that the script to determine the masses of the stars contains two errors. This script and a related one have been used to determine masses of globular cluster stars and distances to field stars in 12 papers published between 1990 and 2014. While the numerical values need to be revised none of the conclusions are affected. We provide the updated numerical values and figures for all 12 publications here. In addition we describe the effects on those refereed publications that used the distances to the field stars.

Key words. stars: horizontal-branch – stars: atmospheres – stars: AGB and post-AGB – globular clusters: general – errata, addenda

1. Introduction

We discovered that the script used in a number of papers by our group to determine the masses of the horizontal branch (HB) stars contains two errors (see Sect. 2.1 for the corrected values). This script was used also to determine masses of hot stars (mostly HB stars) in globular clusters by Moehler et al. (2011, ω Cen, Sect. 2.2), Moehler & Sweigart (2006, NGC 6388, Sect. 2.4), Moehler et al. (2003, M 3 and M 13, Sect. 2.5), Moehler et al. (2000b, NGC 6752, Sect. 2.7), Moehler et al. (2000a, 47 Tuc and NGC 362, Sect. 2.6), Moehler et al. (1998, UV bright stars, Sect. 2.8), Moehler et al. (1997, NGC 6752, Sect. 2.9), Moehler et al. (1995, M 15, Sect. 2.10), and Moni Bidin et al. (2007, NGC 6752, Sect. 2.3), but not for de Boer et al. (1995, NGC 6397).

A similar script with the same errors was used earlier to determine distances for subdwarf B stars in the field of the Milky Way by Theissen et al. (1993, sdB, Sect. 3.1) and Moehler et al. (1990, sdB, Sect. 3.2). The script was not used for Dreizler et al. (1990).

These distances were then used for other research (see Sect. 4): distances to intermediate- and high-velocity clouds by de Boer et al. (1994a, Sect. 4.1), Centurión et al. (1994, Sect. 4.3), Smoker et al. (2004, 2006, Sect. 4.8), kinematic studies by Colin et al. (1994, Sect. 4.2), de Boer et al. (1997, Sect. 4.4), Geffert (1998, Sect. 4.5), and Altmann et al. (2004, Sect. 4.7), and also to study resolved sdB binaries (Heber et al. 2002, Sect. 4.6).

These scripts were derived from Eq. (1)

$$\frac{R_*^2}{d_*^2} = \frac{F_{\rm obs}}{F_{\rm th}}/\pi, \tag{1}$$

which can be translated to

$$\log d_* = 0.5 \cdot (-\log g_* + 0.4 \cdot (V_* - A_V - V_{\rm th}) + C1), \tag{2}$$

with

$$C1 = \log g_\odot + \log \frac{M_*}{M_\odot} + 2 \cdot \log R_\odot - \log F_{V=0} + \log \pi, \tag{3}$$

(assuming a const. mass of $M_* = 0.5 \cdot M_\odot$) or to

$$\log \frac{M_*}{M_\odot} = \log g_* + 0.4 \cdot [(m - M)_0 - V_* + A_V + V_{\rm th}] - C2, \tag{4}$$

with

$$C2 = \log g_\odot + 2 \cdot \log R_\odot - \log F_{V=0} + \log \pi - 2 = C1 - \log \frac{M_*}{M_\odot} - 2. \tag{5}$$

As $V_{\rm th}$ in these equations we used the V magnitude tabulated by Kurucz (1992). When first doing so we noticed that the distances derived that way were about 2.5 times larger than the ones obtained using bolometric corrections. The Kurucz flux values are measured per nm, while the flux at $V = 0$ is given per Å. Assuming that the fluxes were integrated and not averaged across the wavelength interval we added $1\overset{\rm m}{.}0$ to the $V_{\rm th}$ values to correct this difference in binning, while $2\overset{\rm m}{.}5$ would have been required for a factor of ten.

Once we found that error we used instead the following equations to determine masses and distance together with the bolometric corrections from Flower (1996)

$$\log \frac{M_*}{M_\odot} = \log \frac{g_*}{g_\odot} - 4 \cdot \log \frac{T_*}{T_\odot} - \frac{M_V + BC - 4.74}{2.5}, \tag{6}$$

which can be rewritten to

$$\log \frac{M_*}{M_\odot} = \log g_* + 0.4 \cdot [(m - M)_0 - V_* + A_V - BC] - 4 \cdot \log T_* + C3, \tag{7}$$

with

$$C3 = -\log g_\odot + 4 \cdot \log T_\odot + \frac{4.74}{2.5}. \tag{8}$$

The equation for the distances then becomes

$$\log d_* = 2 \cdot \log T_* - 0.5 \cdot \log g_* + 0.2 \cdot (V_* - A_V + BC) + C4, \tag{9}$$

with

$$C4 = 0.5 \cdot (\log \frac{M}{M_\odot} - C3) + 1, \tag{10}$$

(again assuming a const. mass of $M_* = 0.5 \cdot M_\odot$)

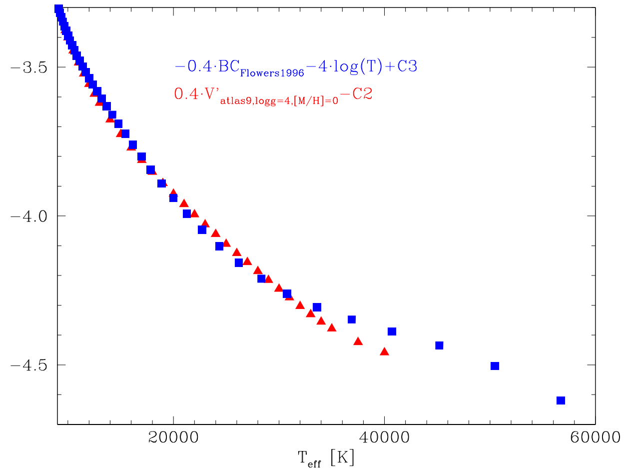

Fig. 1. Values of $-0.4 \cdot BC - 4 \cdot \log T_* + C3$ from Eq. (7) and $0.4 \cdot V'_{\rm th} - C2$ from Eq. (4) for [M/H] = 0 and $\log g = 4.5$ vs. effective temperature (with $V'_{\rm th} = V_{\rm th} + 1$).

For stars between 7943 K and 56 728 K (the hottest star in Flower 1996) we fitted a 5th polynomial to the bolometric corrections versus effective temperature. For hotter stars we extrapolated a 4th polynomial fitted for the temperature range $10\,000\,{\rm K} \leq T_{\rm eff} \leq 56\,728\,{\rm K}$, which proved to be more robust at the hot end.

As one can see, the terms relating to the surface gravity, visual brightness, distance, or mass are the same in the equations using the theoretical visual magnitude or using bolometric corrections. In Fig. 1 we show the terms $-0.4 \cdot BC - 4 \cdot \log T_* + C3$ from Eq. (7) and $0.4 \cdot V'_{\rm th} - C2$ from Eq. (4) for [M/H] = 0 and $\log g = 4.5$ versus effective temperature (with $V'_{\rm th} = V_{\rm th} + 1$).

Figure 1 illustrates that the differences are very small, as already seen in the comparison of masses derived both ways in Moni Bidin et al. (2007, their Fig. 7).

In the following sections we will present the revised masses and distances for the stars studied including some revised diagrams and revised tables. The title of each subsection refers to the publication in question.

2. Masses of hot stars in globular clusters

The publications discussed in this section determine effective temperatures, surface gravities, and helium abundances of hot stars in globular clusters and derive their masses from the known apparent brightnesses, reddenings, and distances. Most of them deal with horizontal branch stars, except for Moehler et al. (1998), which analyses UV-bright stars. Moehler et al. (2014, 2003, 2000b) also provide estimates of some metal abundances.

2.1. *Moehler et al. (2014, NGC 288)*

See Figs. 2 and 3.

On average the mass values according to Eq. (6) are (3.2 ± 6.5)% higher than the original ones for homogeneous model atmospheres and (9.4 ± 3.4)% higher for stratified model atmospheres (applying the same offset to the bolometric corrections as we applied to $V_{\rm th}$ in the original paper). The conclusions are not affected by this change. Figure 2 contains the corrected values for Moehler et al. (2011, Sect 2.2) and Moni Bidin et al. (2007, Sect. 2.3).

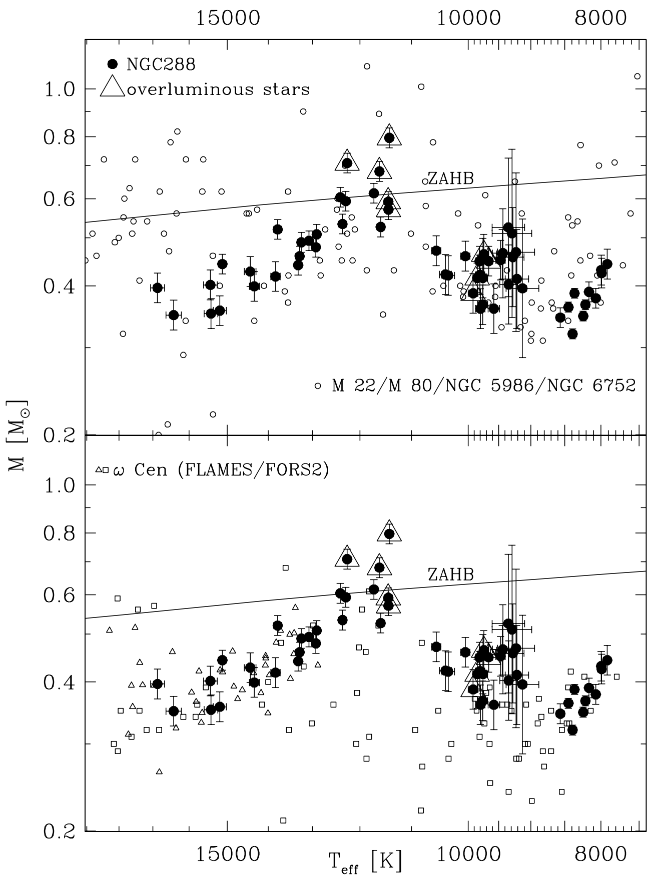

Fig. 2. Figure to replace Fig. 6 in Moehler et al. (2014, NGC 288). Masses from line profile fits. For comparison we also show a canonical zero-age horizontal branch from Moehler et al. (2003). In the *upper plot* we also show results from FORS2 observations of hot HB stars in M 80, NGC 5986 (Moni Bidin et al. 2009), NGC 6752 (Moni Bidin et al. 2007), and M 22 (Salgado et al. 2013). In the *lower plot* we also provide the results obtained from FLAMES and FORS2 observations of hot horizontal branch stars in ω Cen (Moehler et al. 2011, small squares; Moni Bidin et al. 2011, small triangles).

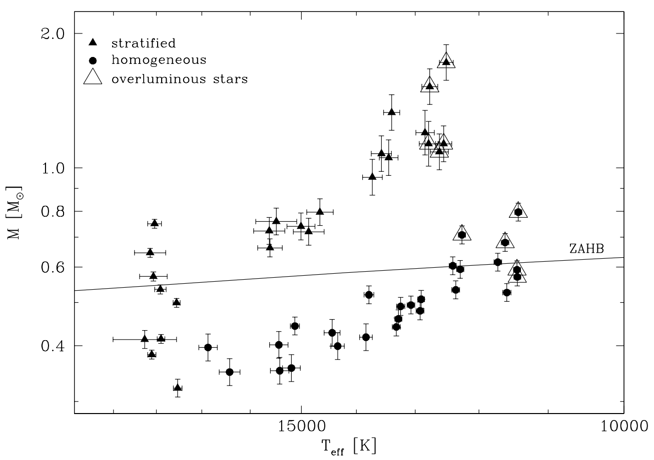

Fig. 3. Figure to replace Fig. 11 in Moehler et al. (2014, NGC 288). Masses determined from line profile fits for stars bluer than the Grundahl jump, using homogeneous (filled circles) and stratified (filled triangles) model spectra.

2.2. Moehler et al. (2011, ω Cen)

See Fig. 4.

The mass values according to Eq. (6) are on average $(8.7 \pm 2.6)\%$ higher than the original ones for the cool stars in Group1, $(6.9 \pm 11.1)\%$ lower for the hot stars in Group1, and $(3.2 \pm 8.0)\%$ lower for the stars in Group2. For the hot stars in Group1 and the stars in Group2 we had used metal-poor theoretical magnitudes in the original paper. The conclusions are not affected.

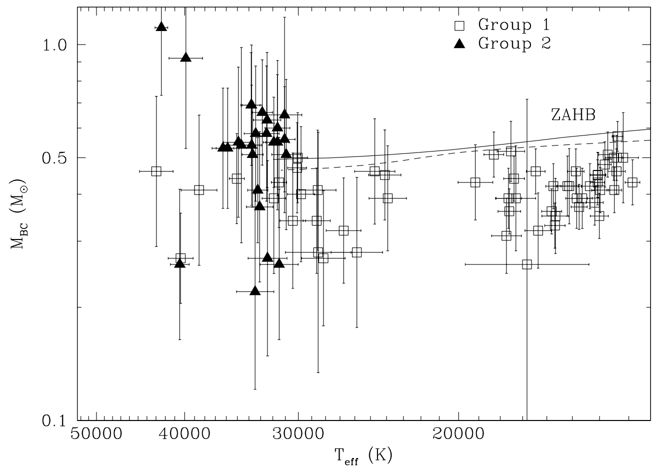

Fig. 4. Figure to replace Fig. 7 in Moehler et al. (2011, ω Cen). The effective temperatures and masses derived for our target stars (formal errors multiplied by two, see text [original paper] for details). Helium-poor and helium-rich stars are marked by open squares and filled triangles, respectively. The stars with super-solar helium abundances are shown with the parameters derived from models without C/N enhancement. The lines mark the zero-age horizontal branch for $Y = 0.23$ (solid) and 0.38 (dashed, see text [original paper] for details).

2.3. Moni Bidin et al. (2007, NGC 6752)

See Fig. 5 and Table 1.

On average the mass values according to Eq. (6) are $(11.3 \pm 2.7)\%$ higher than the original ones for effective temperatures between 11 000 K and 18 000 K and $(2.8 \pm 2.2)\%$ lower for lower and higher effective temperatures. This effect is discussed already in the original paper and its conclusions are not affected.

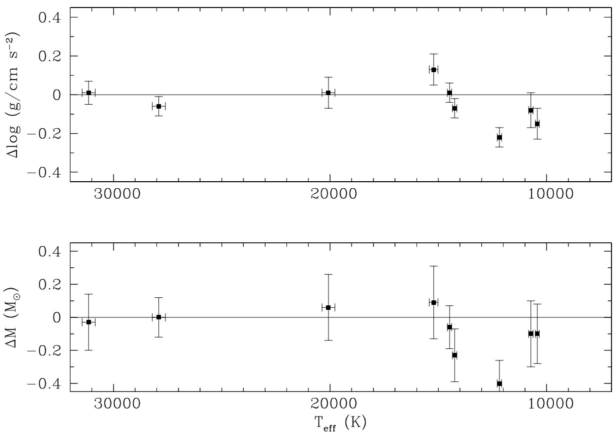

Fig. 5. Figure to replace Fig. 6 in Moni Bidin et al. (2007, NGC 6752). Differences of surface gravities and derived masses between this work and Moehler et al. (2000b) for the nine stars in common. The errors are the quadratic sum of the ones for each set of data. The difference is in the sense (our) – (M00).

Figure 7 of Moni Bidin et al. (2007) shows the mass values according to Eq. (4) in its upper panel and the mass values according to Eq. (6) in its lower panel. Therefore we do not provide an updated version of this figure here.

Table 1. Table to replace Table 1 in Moni Bidin et al. (2007, NGC 6752). Atmospheric parameters and derived masses for target stars.

ID	$T_{\rm eff}$ (K)	$\log g$	$\log \frac{N_{\rm He}}{N_{\rm H}}$	M ($M_\odot$)	
14770	28 400 ± 300	5.53 ± 0.03	−2.25 ± 0.05	0.55 ± 0.04	
11634	9700 ± 100	3.39 ± 0.05	−1.00 ± 0.00	0.37 ± 0.04	
14944	14 500 ± 100	4.27 ± 0.03	−2.29 ± 0.09	0.56 ± 0.04	
15026	8700 ± 100	3.08 ± 0.05	−1.00 ± 0.00	0.35 ± 0.03	
16551	14 500 ± 100	4.28 ± 0.03	−2.31 ± 0.09	0.57 ± 0.04	
15395	25 700 ± 300	5.58 ± 0.03	−2.54 ± 0.05	0.66 ± 0.06	□
20919	8000 ± 40	2.91 ± 0.03	−1.00 ± 0.00	0.37 ± 0.03	
18782	12 100 ± 100	3.78 ± 0.03	−2.10 ± 0.12	0.53 ± 0.04	
17941	24 800 ± 400	5.02 ± 0.03	−1.98 ± 0.05	0.71 ± 0.06	*
20302	19 100 ± 300	4.87 ± 0.03	−1.78 ± 0.03	0.43 ± 0.03	
26756	10 430 ± 90	3.55 ± 0.03	−1.00 ± 0.00	0.39 ± 0.03	
27181	13 500 ± 100	3.96 ± 0.03	−1.98 ± 0.09	0.43 ± 0.03	△
24849	11 860 ± 90	4.09 ± 0.03	−1.65 ± 0.09	1.10 ± 0.03	
27604	17 600 ± 200	4.60 ± 0.02	−1.89 ± 0.03	0.51 ± 0.08	
28231	26 900 ± 300	5.58 ± 0.03	−1.84 ± 0.03	0.61 ± 0.05	□
26760	15 600 ± 200	4.42 ± 0.03	−1.93 ± 0.07	0.62 ± 0.05	
28554	26 500 ± 400	5.59 ± 0.03	−2.33 ± 0.05	0.66 ± 0.06	□
28693	28800 ± 400	5.56 ± 0.03	−3.26 ± 0.02	0.55 ± 0.04	
28947	22 100 ± 400	5.17 ± 0.03	−1.84 ± 0.02	0.55 ± 0.04	
4964	10 740 ± 100	3.72 ± 0.03	−1.00 ± 0.00	0.58 ± 0.05	
49317	7790 ± 30	2.56 ± 0.03	−1.00 ± 0.00	0.18 ± 0.01	
5455	26 600 ± 300	5.63 ± 0.03	−2.23 ± 0.02	0.66 ± 0.06	□
5487	20 000 ± 300	5.09 ± 0.03	−1.60 ± 0.02	0.56 ± 0.05	
5134	15 200 ± 200	4.33 ± 0.03	−2.42 ± 0.10	0.48 ± 0.04	
4672	25 200 ± 300	5.39 ± 0.03	−2.04 ± 0.03	0.50 ± 0.04	
5201	27 900 ± 300	5.53 ± 0.03	−1.58 ± 0.03	0.41 ± 0.03	
5865	27 800 ± 300	5.53 ± 0.03	−3.07 ± 0.05	0.57 ± 0.05	□
7843	14 100 ± 200	4.07 ± 0.03	−2.01 ± 0.07	0.36 ± 0.03	△
6284	27 200 ± 300	5.41 ± 0.03	−2.27 ± 0.03	0.47 ± 0.04	
10257	8800 ± 200	3.06 ± 0.09	−1.00 ± 0.00	0.30 ± 0.03	
10625	28 700 ± 300	5.67 ± 0.03	−1.84 ± 0.03	0.50 ± 0.04	
8672	30 100 ± 300	5.73 ± 0.03	−2.90 ± 0.09	0.47 ± 0.04	
10711	27 700 ± 300	5.63 ± 0.03	−2.28 ± 0.05	0.60 ± 0.05	□
11609	14 300 ± 100	4.23 ± 0.02	−3.04 ± 0.16	0.58 ± 0.04	
14664	8050 ± 40	3.02 ± 0.03	−1.00 ± 0.00	0.42 ± 0.03	
14727	10 600 ± 100	3.72 ± 0.03	−1.00 ± 0.00	0.79 ± 0.06	
35186	10 800 ± 100	3.73 ± 0.03	−1.00 ± 0.00	0.66 ± 0.05	
35662	12 900 ± 200	3.96 ± 0.03	−2.15 ± 0.16	0.48 ± 0.03	
35499	12 500 ± 100	3.96 ± 0.03	−2.09 ± 0.12	0.59 ± 0.04	
36242	12 800 ± 100	3.93 ± 0.03	−2.03 ± 0.10	0.46 ± 0.03	
36480	22 400 ± 400	5.16 ± 0.03	−1.98 ± 0.02	0.47 ± 0.04	
36502	12 300 ± 100	3.89 ± 0.03	−1.92 ± 0.10	0.52 ± 0.04	
36830	27 400 ± 300	5.63 ± 0.03	−2.08 ± 0.05	0.61 ± 0.05	□
38095	14 300 ± 200	4.03 ± 0.03	−1.93 ± 0.05	0.35 ± 0.02	△
38087	27 300 ± 300	5.53 ± 0.03	−2.18 ± 0.05	0.62 ± 0.05	□
32470	10 620 ± 90	3.59 ± 0.03	−1.00 ± 0.00	0.40 ± 0.03	
28695	9600 ± 100	3.35 ± 0.07	−1.00 ± 0.00	0.38 ± 0.04	
38504	12 200 ± 100	3.90 ± 0.03	−2.13 ± 0.10	0.54 ± 0.05	
39008	30 900 ± 300	5.55 ± 0.03	−2.29 ± 0.05	0.55 ± 0.05	
38889	12 700 ± 200	3.94 ± 0.05	−2.00 ± 0.17	0.52 ± 0.04	
38963	9000 ± 200	3.16 ± 0.09	−1.00 ± 0.00	0.31 ± 0.04	

2.4. Moehler et al. (2006, NGC 6388)

See Fig. 6.

On average the mass values according to Eq. (6) are (4.1 ± 5.9)% higher than the original ones. The conclusions are not affected by this change.

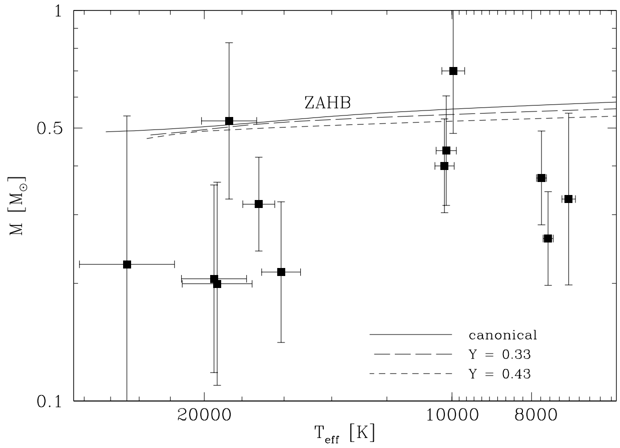

Fig. 6. Figure to replace Fig, 6 in Moehler & Sweigart (2006, NGC 6388). Effective temperatures and masses for our target stars. For comparison we show both the canonical ZAHB (Y = 0.23, solid line) and two helium-rich ZAHBs (Y = 0.33, long dashed line; Y = 0.43, short dashed line).

2.5. Moehler et al. (2003, M 3 and M 13)

See Fig. 7.

On average the mass values according to Eq. (6) are (3.1 ± 0.9)% lower than the original ones for stars cooler than 12 000 K and (9.3 ± 3.6)% higher for the hotter stars. The conclusions are not affected by this change.

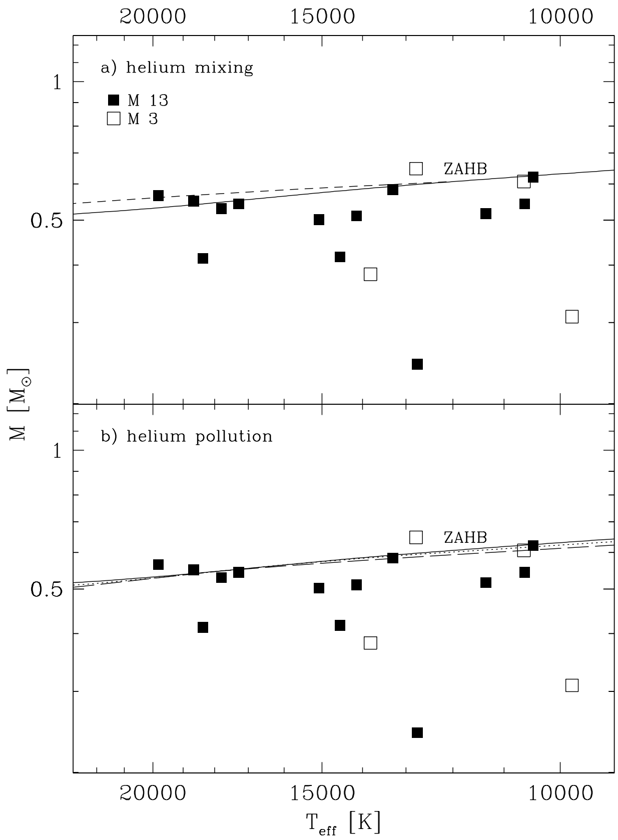

Fig. 7. Figure to replace Fig. 9 in Moehler et al. (2003, M 3 and M 13). Temperatures and masses of the programme stars in M 3 and M 13 (from metal-rich model atmospheres for stars hotter than 12 000 K and metal-poor model atmospheres for cooler stars; in both cases metal lines were included in the theoretical spectra) compared to evolutionary tracks. *a)* The solid line marks the canonical ZAHB and the mixed ZAHB is given by the short-dashed line (see Sect. 6.1 [of the original paper] for details). *b)* Again the solid line marks the canonical ZAHB and the polluted ZAHBs are given by the dotted (Y = 0.28) and long-dashed line (Y = 0.33), respectively (see Sect. 6.2 [of the original paper] for details).

2.6. Moehler et al. (2000a, 47 Tuc and NGC 362)

See Table 2.

On average the mass values according to Eq. (6) are $(0.2 \pm 7.6)\%$ lower than the original ones. The new masses of the probable SMC members *MJ65* (9.2 $M_\odot$), *MJ94* (7.4 $M_\odot$), and *MJ5381* (5.7 $M_\odot$) are now slightly closer to their evolutionary masses of 7 $M_\odot$, 4 $M_\odot$, and 5 $M_\odot$, respectively. The conclusions are not affected by these changes.

Table 2. Table to replace Table 2 in Moehler et al. (2000a, 47 Tuc and NGC 362). Atmospheric parameters and masses for the programme stars as derived from low and medium resolution spectroscopic data. The surface gravities derived from the low resolution spectrophotometric data are rather uncertain. We also give the reduced χ^2 values from the line profile fits and the errors listed below are the rms errors of the fit routine adjusted as described in the text [original paper]. The three rightmost columns give the cluster resp. SMC membership according to the radial velocity, proper motion, and derived mass of the star (see Sect. 5 [of the original paper] for details). A – means that the information places a star neither to the globular cluster nor to the SMC. Brackets note dubious assignments.

Star	Spectrophotometry			Medium resolution data			Masses		Membership		
	$T_{\rm eff}$ (K)	$\log g$ (cm/s^2)	χ^2	$T_{\rm eff}$ (K)	$\log g$ (cm/s^2)	$\log \frac{n_{\rm He}}{n_{\rm H}}$	cluster ($M_\odot$)	SMC ($M_\odot$)	$v_{\rm rad}$	proper motion	mass
				47Tuc							
MJ280	13 500	4.0:	2.75	$14\,500 \pm 290$	4.21 ± 0.08	-1.41 ± 0.16	0.66	134	C	C	C
MJ8279	18 000	4.5:	1.96	$18\,500 \pm 530$	4.20 ± 0.10	-1.56 ± 0.11	0.02	3.6	SMC		SMC
MJ33410	10 000	3.5:	4.53	$10\,400 \pm 210$	3.53 ± 0.11	-1.00	0.51	104	C		C
MJ38529	8000[1]	3.0:	2.25	7950 ± 20	5.21 ± 0.05	-1.00	22	4400	C	C	–
	12 500[2]	3.5:	7.85	$14\,000 \pm 400$	5.34 ± 0.11	<-2	8.3	1700	C	C	–
				NGC 362							
MJ65	8500	2.5:	2.03	9460 ± 540	2.46 ± 0.32	-1.00	0.16	9.2	SMC	–	SMC
MJ94	11 000	3.5:	3.53	$11\,700 \pm 350$	3.33 ± 0.11	-1.93 ± 0.35	0.13	7.4	SMC	–	SMC
MJ2341	16 000	4.5:	2.08	$17\,400 \pm 500$	3.97 ± 0.10	-1.79 ± 0.13	0.10	5.7	–		SMC
MJ3832			2.64	8250 ± 140	2.77 ± 0.06	-1.00	0.23	13	C		(C)
MJ5381	9000	3.0:	2.43	7780 ± 100	2.14 ± 0.05	-1.00	0.04	2.2	(SMC)	–	–
MJ6558			3.06	$12\,500 \pm 350$	4.09 ± 0.11	-1.61 ± 0.40	1.08	64	C	–	(C)
MJ8241	8500	3.5:	3.49	7980 ± 50	3.06 ± 0.06	-1.00	0.52	30	C		C
MJ8453[3]	14000	4.0:	1.53	$16\,600 \pm 560$	4.11 ± 0.11	-1.99 ± 0.11	0.27	16	–	–	(C)

Notes. [(1)] Fitting the continuum; [(2)] fitting the Balmer jump; [(3)] H_β, H_γ are not included in the fit of *MJ8453*.

2.7. Moehler et al. (2000b, NGC 6752)

See Fig. 8 and Tables 3–7.

We summarise the average ratios between mass values derived using Eqs. (6) and (4), respectively, in Table 3. The different ratios found for different model atmosphere metallicities reflect also the fact that we used theoretical V_{th} magnitudes of the same metallicity as the model atmospheres, while the bolometric corrections are not distinguished by metallicity.

Table 3. Average ratio between mass values derived using Eqs. (6) and (4), respectively, for the different metallicities of model atmospheres used for the analysis and the two temperature ranges below and above 12 000 K.

[M/H]	$T_{\rm eff}$ < 20 000 K	$T_{\rm eff}$ ≥ 20 000 K
−1.5	0.963 ± 0.031	0.872 ± 0.034
+0.0	1.042 ± 0.026	0.954 ± 0.029
+0.5	1.109 ± 0.028	0.999 ± 0.041

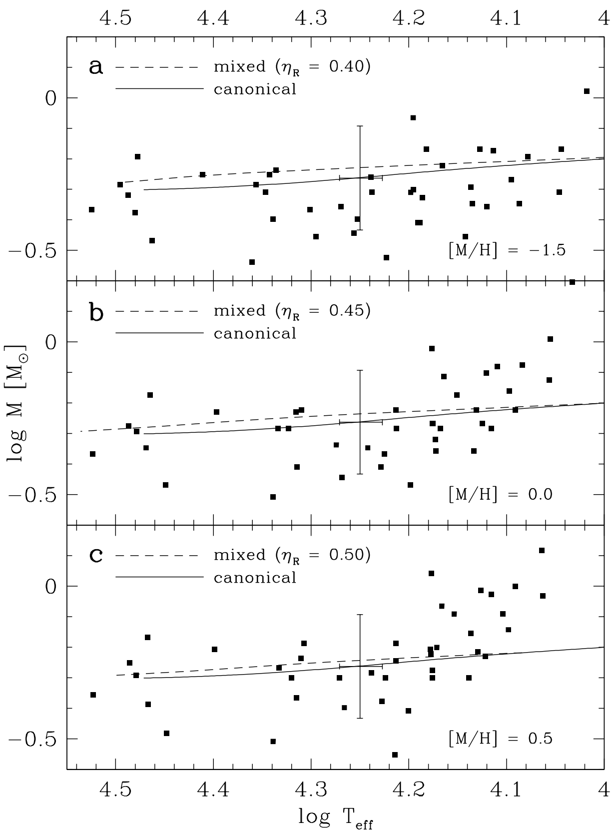

Fig. 8. Figure to replace Fig. 7a–c in Moehler et al. (2000b, NGC 6752). Temperatures and masses (derived from Buonanno et al.'s photometry) of the programme stars in NGC 6752. *a)* Determined using model atmospheres with cluster metallicity ([M/H] = −1.5), *b)* adopting a solar metallicity ([M/H] = 0) for the model atmospheres, *c)* adopting a super–solar metallicity ([M/H] = +0.5) for the model atmospheres. For more details see Sect. 4.1 [of the original paper]. The dashed resp. solid lines mark the ZAHB masses for a metallicity [M/H] = −1.54, as computed with and without mixing, respectively. (see Sect. 4.2 and Fig. 4 [of the original paper] for details).

Table 4. Table to replace Table 2 in Moehler et al. (2000b, NGC 6752). Physical parameters, helium abundances, and masses for the target stars in NGC 6752 as derived using metal-poor model atmospheres. We used the photometry of Buonanno et al. (1986) to derive the masses.

Star	$T_{\rm eff}$ (K)	$\log g$ (cm s^{-2})	$\log \frac{n_{\rm He}}{n_{\rm H}}$	M ($M_\odot$)
ESO 1.52 m telescope observations in 1998				
652	12 500 ± 310	3.86 ± 0.09	−2.00 ± 0.35	0.54
1132	17 300 ± 520	4.31 ± 0.09	−2.46 ± 0.16	0.49
1152	15 700 ± 360	4.19 ± 0.05	−2.57 ± 0.17	0.50
1157	15 800 ± 460	4.14 ± 0.09	−2.89 ± 0.31	0.49
1738	16 700 ± 700	4.15 ± 0.12	−2.24 ± 0.28	0.30
2735	11 100 ± 260	3.78 ± 0.12	−1.14 ± 0.36	0.68
3253	13 700 ± 390	3.80 ± 0.09	−2.41 ± 0.29	0.50
3348	12 000 ± 270	3.73 ± 0.07	−2.18 ± 0.38	0.64
3408	14 600 ± 400	4.21 ± 0.09	−2.40 ± 0.36	0.60
3410	15 500 ± 460	4.14 ± 0.09	−2.22 ± 0.19	0.39
3424	17 900 ± 570	4.23 ± 0.09	−2.60 ± 0.21	0.40
3450	13 200 ± 290	3.84 ± 0.07	−2.05 ± 0.24	0.44
3461	15 200 ± 500	4.18 ± 0.09	≤−3	0.68
3655	25 800 ± 1300	5.15 ± 0.16	−2.32 ± 0.24	0.56
3736	13 400 ± 370	3.91 ± 0.09	−1.84 ± 0.17	0.68
4172	12 200 ± 260	3.68 ± 0.07	−2.24 ± 0.54	0.45
4424	13 000 ± 290	3.99 ± 0.07	−2.36 ± 0.38	0.67
4551	15 400 ± 530	3.96 ± 0.09	−2.21 ± 0.24	0.39
4822	13 900 ± 450	3.91 ± 0.09	−2.24 ± 0.28	0.35
4951	17 300 ± 580	4.38 ± 0.09	−2.63 ± 0.22	0.55
ESO NTT observations in 1997				
944	11 100 ± 230	3.70 ± 0.10	−0.84 ± 0.31	0.49
1391	19 700 ± 570	4.49 ± 0.09	−2.04 ± 0.10	0.35
1780	18 000 ± 580	4.40 ± 0.09	−2.31 ± 0.14	0.36
2099	20 000 ± 820	4.61 ± 0.12	−2.38 ± 0.22	0.43
ESO NTT observations in 1998				
2697	15 700 ± 400	4.08 ± 0.07	−2.36 ± 0.17	0.86
2698	15 400 ± 610	4.11 ± 0.10	−2.07 ± 0.28	0.47
2747	22 700 ± 650	4.85 ± 0.09	−2.16 ± 0.10	0.52
2932	18 600 ± 700	4.63 ± 0.12	−1.57 ± 0.12	0.44
3006	30 000 ± 640	5.19 ± 0.09	≤−3	0.64
3094	10 400 ± 120	3.81 ± 0.17	−1.83 ± 1.35	1.05
3140[1]	8000 ± 100	2.84 ± 0.14	−1.00 ± 0.00	0.31
3253	13 700 ± 470	3.75 ± 0.10	−1.85 ± 0.31	0.45
3699	22 900 ± 990	4.64 ± 0.12	−2.29 ± 0.10	0.29
ESO NTT observations in 1993				
491	29 000 ± 520	5.41 ± 0.07	≤−3	0.34
916	30 200 ± 430	5.61 ± 0.07	−1.71 ± 0.05	0.42
1509	17 400 ± 630	4.10 ± 0.10	−2.17 ± 0.16	0.25
1628	21 800 ± 590	4.83 ± 0.09	−2.53 ± 0.12	0.40
2162	33 400 ± 390	5.78 ± 0.07	−1.94 ± 0.09	0.43
2395	22 200 ± 690	5.10 ± 0.09	−1.78 ± 0.07	0.49
3915	31 300 ± 510	5.55 ± 0.09	≤−3	0.52
3975	21 700 ± 460	4.97 ± 0.07	−2.04 ± 0.10	0.58
4009	30 700 ± 920	5.61 ± 0.12	≤−3	0.48
4548	22 000 ± 1380	5.11 ± 0.19	−2.02 ± 0.16	0.56

Notes. [1] This star is omitted from further analysis as it lies in a temperature range that is difficult to analyse and not of great interest for our discussion.

Table 5. Table to replace Table 3 in Moehler et al. (2000b, NGC 6752). Physical parameters, helium abundances, and masses for the target stars in NGC 6752 as derived using solar metallicity model atmospheres.

Star	$T_{\rm eff}$ (K)	$\log g$ (cm s^{-2})	$\log \frac{n_{\rm He}}{n_{\rm H}}$	M ($M_\odot$)
ESO 1.52 m telescope observations in 1998				
652	12 500 ± 230	3.98 ± 0.07	−2.19 ± 0.36	0.69
1132	16 300 ± 460	4.31 ± 0.07	−2.45 ± 0.16	0.52
1152	15 000 ± 290	4.21 ± 0.05	−2.58 ± 0.17	0.54
1157	15 000 ± 360	4.15 ± 0.07	−2.89 ± 0.31	0.54
1738	15 800 ± 580	4.15 ± 0.10	−2.23 ± 0.28	0.34
2735	11 400 ± 170	3.96 ± 0.07	−1.51 ± 0.28	1.02
3253	13 500 ± 310	3.88 ± 0.07	−2.57 ± 0.28	0.60
3348	12 100 ± 220	3.86 ± 0.07	−2.44 ± 0.38	0.84
3408	14 100 ± 330	4.24 ± 0.07	−2.47 ± 0.36	0.67
3410	14 900 ± 370	4.17 ± 0.07	−2.25 ± 0.19	0.48
3424	16 800 ± 510	4.21 ± 0.09	−2.58 ± 0.22	0.43
3450	13 000 ± 210	3.92 ± 0.05	−2.22 ± 0.24	0.52
3461	14 600 ± 400	4.20 ± 0.09	≤−3	0.77
3655	24 900 ± 1250	5.14 ± 0.16	−2.32 ± 0.24	0.59
3736	13 200 ± 270	3.99 ± 0.07	−1.98 ± 0.17	0.79
4172	12 300 ± 200	3.81 ± 0.05	−2.49 ± 0.55	0.60
4424	12 900 ± 210	4.07 ± 0.05	−2.58 ± 0.40	0.83
4551	14 900 ± 410	3.99 ± 0.09	−2.26 ± 0.24	0.44
4822	13 600 ± 350	3.97 ± 0.09	−2.37 ± 0.28	0.44
4951	16 300 ± 520	4.38 ± 0.09	−2.61 ± 0.22	0.60
ESO NTT observations in 1997				
944	11 400 ± 190	3.90 ± 0.09	−1.27 ± 0.22	0.75
1391	18 500 ± 570	4.45 ± 0.09	−2.02 ± 0.10	0.36
1780	16 900 ± 530	4.37 ± 0.09	−2.28 ± 0.14	0.39
2099	18 800 ± 790	4.58 ± 0.10	−2.36 ± 0.22	0.46
ESO NTT observations in 1998				
2697	15 000 ± 360	4.10 ± 0.07	−2.39 ± 0.17	0.95
2698	14 700 ± 490	4.13 ± 0.10	−2.10 ± 0.26	0.52
2747	21 600 ± 700	4.80 ± 0.09	−2.16 ± 0.10	0.52
2932	17 500 ± 600	4.61 ± 0.10	−1.54 ± 0.10	0.45
3006	29 100 ± 740	5.18 ± 0.09	≤−3	0.67
3094	10 800 ± 310	4.01 ± 0.14	−2.33 ± 1.97	1.57
3253	13 300 ± 370	3.81 ± 0.09	−1.95 ± 0.31	0.54
3699	21 800 ± 1050	4.60 ± 0.12	−2.30 ± 0.10	0.31
ESO NTT observations in 1993				
491	28 100 ± 540	5.40 ± 0.07	≤−3	0.34
916	29 400 ± 480	5.60 ± 0.07	−1.70 ± 0.05	0.45
1509	16 400 ± 510	4.07 ± 0.09	−2.15 ± 0.16	0.25
1628	20 600 ± 620	4.78 ± 0.09	−2.52 ± 0.12	0.39
2162	33 400 ± 460	5.79 ± 0.07	−1.92 ± 0.09	0.43
2395	21 000 ± 750	5.06 ± 0.10	−1.78 ± 0.09	0.52
3915	30 700 ± 620	5.54 ± 0.09	≤−3	0.53
3975	20 400 ± 520	4.92 ± 0.07	−2.02 ± 0.12	0.60
4009	30 100 ± 1120	5.60 ± 0.14	≤−3	0.51
4548	20 700 ± 1490	5.06 ± 0.19	−2.00 ± 0.17	0.59

Table 6. Table to replace Table 5 in Moehler et al. (2000b, NGC 6752). Physical parameters, helium abundances, and masses for the target stars in NGC 6752 as derived using metal-rich model atmospheres.

Star	$T_{\rm eff}$ (K)	$\log g$ (cm s^{-2})	$\log \frac{n_{\rm He}}{n_{\rm H}}$	M ($M_\odot$)
ESO 1.52 m telescope observations in 1998				
652	12 700 ± 220	4.05 ± 0.07	−2.40 ± 0.36	0.81
1132	16 300 ± 430	4.36 ± 0.07	−2.55 ± 0.14	0.57
1152	15 100 ± 290	4.26 ± 0.05	−2.71 ± 0.16	0.62
1157	15 100 ± 370	4.20 ± 0.07	−2.98 ± 0.26	0.60
1738	15 900 ± 540	4.21 ± 0.10	−2.37 ± 0.26	0.39
2735	11 600 ± 180	4.08 ± 0.07	−1.74 ± 0.24	1.31
3253	13 700 ± 300	3.94 ± 0.07	−2.76 ± 0.24	0.70
3348	12 300 ± 210	3.94 ± 0.07	−2.65 ± 0.36	1.00
3408	14 200 ± 310	4.30 ± 0.07	−2.64 ± 0.35	0.81
3410	15 000 ± 350	4.23 ± 0.07	−2.40 ± 0.19	0.53
3424	16 700 ± 490	4.24 ± 0.09	−2.66 ± 0.21	0.50
3450	13 200 ± 200	3.99 ± 0.05	−2.45 ± 0.26	0.59
3461	14 700 ± 380	4.26 ± 0.09	−3.37 ± 0.33	0.86
3655	25 000 ± 170	5.16 ± 0.16	−2.31 ± 0.24	0.62
3736	13 400 ± 260	4.07 ± 0.07	−2.17 ± 0.17	0.97
4172	12 500 ± 200	3.88 ± 0.05	−2.70 ± 0.50	0.72
4424	13 000 ± 210	4.13 ± 0.05	−2.79 ± 0.35	0.94
4551	15 000 ± 400	4.05 ± 0.09	−2.43 ± 0.24	0.50
4822	13 800 ± 340	4.04 ± 0.09	−2.59 ± 0.28	0.50
4951	16 300 ± 480	4.42 ± 0.09	−2.72 ± 0.21	0.65
ESO NTT observations in 1997				
944	11 600 ± 180	4.00 ± 0.07	−1.52 ± 0.19	0.93
1391	18 400 ± 580	4.48 ± 0.09	−2.08 ± 0.10	0.40
1780	16 900 ± 500	4.41 ± 0.09	−2.37 ± 0.12	0.42
2099	18 700 ± 810	4.60 ± 0.10	−2.41 ± 0.22	0.50
ESO NTT observations in 1998				
2697	15 000 ± 330	4.14 ± 0.07	−2.52 ± 0.17	1.10
2698	14 800 ± 490	4.20 ± 0.10	−2.25 ± 0.28	0.63
2747	21 500 ± 830	4.81 ± 0.09	−2.17 ± 0.10	0.54
2932	17 300 ± 570	4.65 ± 0.10	−1.61 ± 0.10	0.52
3006	29 300 ± 590	5.19 ± 0.07	−3.01 ± 0.31	0.68
3094	11 100 ± 290	4.14 ± 0.10	−2.54 ± 1.97	2.03
3253	13 500 ± 350	3.87 ± 0.09	−2.12 ± 0.31	0.61
3699	21 800 ± 030	4.61 ± 0.12	−2.31 ± 0.10	0.31
ESO NTT observations in 1993				
491	28 000 ± 520	5.40 ± 0.07	−3.40 ± 0.14	0.33
916	29 300 ± 460	5.59 ± 0.05	−1.70 ± 0.05	0.41
1509	16 400 ± 500	4.11 ± 0.09	−2.25 ± 0.16	0.28
1628	20 700 ± 720	4.81 ± 0.09	−2.55 ± 0.12	0.43
2162	33 400 ± 500	5.78 ± 0.07	−1.91 ± 0.09	0.44
2395	20 900 ± 810	5.07 ± 0.09	−1.80 ± 0.09	0.50
3915	30 600 ± 580	5.54 ± 0.07	−3.19 ± 0.19	0.56
3975	20 300 ± 580	4.94 ± 0.07	−2.06 ± 0.12	0.65
4009	30 100 ± 040	5.62 ± 0.12	−3.14 ± 0.19	0.51
4548	20 400 ± 590	5.06 ± 0.19	−2.03 ± 0.17	0.58

Table 7. Table to replace Table 6 in Moehler et al. (2000b, NGC 6752) Mean mass ratios between spectroscopically derived masses and predicted zero-age HB masses at the same effective temperatures. B 2697, B 3006 and stars cooler than 11 500 K are excluded from this comparison. η_R gives the Reimer's mass loss parameter for the respective ZAHB. We derived the masses using the photometry of Buonanno et al. (1986). The cited errors are standard deviations.

cool HBB stars	hot HBB stars	sdB stars	[M/H]	track
$0.87^{+0.20}_{-0.16}$ (16)	$0.71^{+0.20}_{-0.16}$ (9)	$0.91^{+0.21}_{-0.17}$ (12)	−1.5	canonical HB, variable η_R
$0.83^{+0.19}_{-0.16}$ (16)	$0.65^{+0.18}_{-0.14}$ (9)	$0.83^{+0.19}_{-0.16}$ (12)	−1.5	mixed HB, η_R = 0.40
$1.03^{+0.24}_{-0.19}$ (16)	$0.75^{+0.22}_{-0.17}$ (9)	$0.93^{+0.23}_{-0.18}$ (12)	+0.0	canonical HB, variable η_R
$0.99^{+0.23}_{-0.19}$ (16)	$0.71^{+0.20}_{-0.16}$ (9)	$0.86^{+0.21}_{-0.17}$ (12)	+0.0	mixed HB, η_R = 0.45
$1.19^{+0.30}_{-0.24}$ (16)	$0.83^{+0.24}_{-0.18}$ (9)	$0.94^{+0.24}_{-0.19}$ (12)	+0.5	canonical HB, variable η_R
$1.17^{+0.30}_{-0.24}$ (16)	$0.79^{+0.23}_{-0.18}$ (9)	$0.89^{+0.23}_{-0.18}$ (12)	+0.5	mixed HB, η_R = 0.50

2.8. Moehler et al. (1998, UV bright stars in globular clusters)

See Table 8.

On average the mass values according to Eq. (6) are $(5.2 \pm 8.0)\%$ lower than the original ones for stars cooler than 25 000 K and $(15.1 \pm 3.2)\%$ higher for the hotter stars. The surface gravity required to obtain a mass of $0.55\,M_\odot$ for Y453 changed from 5.65 to 5.63 (Sect. 6.2 [of the original paper]). The conclusions are not affected by these changes.

Table 8. Table to replace Table 2 in Moehler et al. (1998, UV bright stars). List of observed stars and their atmospheric parameters. The metallicities and radial velocities for the clusters are taken from the May 1997 tabulation of Harris (1996).

Cluster	[Fe/H]	$v_{\rm hel,Cl.}$ (km s^{-1})	Star	$T_{\rm eff}$ (K)	$\log g$	$\log \frac{n_{\rm He}}{n_{\rm H}}$	$v_{\rm hel}$ (km s^{-1})	M ($M_\odot$)	Status	$\log\left(\frac{L}{L_\odot}\right)_{UV}$	$\log\left(\frac{L}{L_\odot}\right)_V$
NGC 2808	−1.37	+94	C2946	22 700	4.48	−1.72	+93	0.40	post-EHB		+1.99
			C2947	15 100	3.82	−1.21	+134	0.33	post-EHB		+1.78
			C4594	22 700	4.06	−1.57	+89	0.49	post-EHB	+2.44	+2.41
NGC 6121	−1.20	+70	Y453	58 800	5.15	−0.98	+31	0.18	post-EAGB	+2.61	+2.54
NGC 6723	−1.12	−95	III-60	40 600	4.46	−1.03	−109	0.56	post-EAGB	+2.92	+3.06
			IV-9	20 600	3.34	−0.83	−52	0.29	post-EAGB	+2.82	+2.79
NGC 6752	−1.55	−25	B2004	37 000	5.25	−2.39	0	0.38	post-EHB	+1.94	+1.94

2.9. Moehler et al. (1997, NGC 6752)

See Figs. 9, 10 and Table 9.

On average the mass values according to Eq. (6) are $(5.1 \pm 5.2)\%$ lower than the original ones for stars cooler than 35 000 K and $(17.4 \pm 5.3)\%$ higher for the two hotter stars. We repeat the description of the determination of the average logarithmic mass below with the new values (Sect. 5 of the original paper):

"To determine the mean mass of the sdBs (this paper and Heber et al. (1986)) we took all stars with $T_{\rm eff} > 20\,000$ K, excluding B 617 (due to the strange offset between temperatures from continuum and from line profiles) and the post-EHB stars B 852, B 1754, B 4380, resulting in a total of 16 stars. We then calculated the weighted mean of the logarithmic masses for these stars (the weights being derived from the inverse errors). The mean logarithmic mass for these stars then is −0.330 (=0.467 $M_\odot$). The logarithmic standard deviation is 0.043 dex and the expected mean logarithmic error as derived from the observational errors is 0.054 dex. The mean mass therefore agrees extremely well with the value of 0.488 $M_\odot$ predicted by canonical HB theory for these stars (Dorman et al. 1993) and the standard deviation is less than expected. If we omit the stars observed in 1992 (due to their higher errors) we get a mean logarithmic mass for the remaining 12 stars of −0.356 (=0.44 $M_\odot$), which is somewhat lower than the result above but still in good agreement with theoretical predictions. There is no significant difference between the mean mass for the eleven stars below the gap ($\langle \log M \rangle = -0.333$; $\langle M \rangle = 0.463\ M_\odot$) and the five stars inside the gap region ($\langle \log M \rangle = -0.324$; $\langle M \rangle = 0.474\ M_\odot$); again pointing towards their nature being identical. The five stars above the gap ($V < 16\overset{\rm m}{.}0$, $T_{\rm eff} < 20\,000$ K) have a mean logarithmic mass of −0.523 (=0.299 $M_\odot$) with a logarithmic standard deviation of 0.059 (compared to an expected error of 0.073). Canonical theory would predict for these stars a mean logarithmic mass of −0.256 (=0.554 $M_\odot$) with a scatter of 0.018 dex."

The conclusions are not affected by these changes.

The data for other clusters shown in Fig. 10 are the corrected ones from Sect. 2.10.

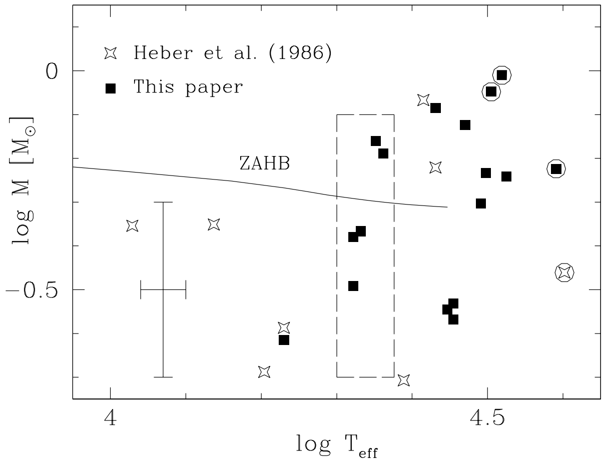

Fig. 9. Figure to replace Fig. 9 in Moehler et al. (1997, NGC 6752). The resulting logarithmic masses listed in Table 3 [original paper, Table 9 here] vs. $\log T_{\rm eff}$. The objects that were not used to derive the mean sdB mass (B 617, B 852, B 1754, B 4380) are marked by circles. Also plotted is the Zero Age HB for [Fe/H] = −1.48 of Dorman et al. (1993). The long dashed line marks the gap region seen in the CMD by Buonanno et al. (1986).

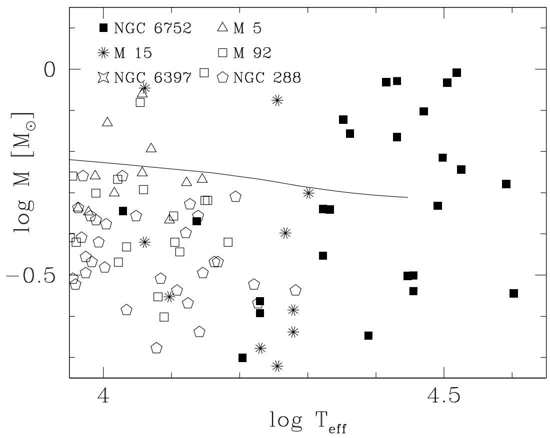

Fig. 10. Figure to replace Fig. 10 in Moehler et al. (1997, NGC 6752). The resulting masses plotted in Fig. 9 [original paper, Fig. 9 here] compared to masses of BHB stars in other clusters. The BHB data are taken from Paper I (Moehler et al. 1995, M 15), II (de Boer et al. 1995, NGC 6397), and Crocker et al. (1988, M 5, M 92, and NGC 288)

Table 9. Table to replace Table 3 in Moehler et al. (1997, NGC 6752). Physical parameters of the observed stars. The star numbers and V, $B-V$ data are taken from Buonanno et al. (1986), except for 3-118, whose data were obtained from Caloi et al. (1986).

Star	V (mag)	$B-V$ (mag)	$T_{\rm eff,UV}$ (K)	$T_{\rm eff,opt.}$ (K)	$T_{\rm eff,lines}$ (K)	$T_{\rm eff,fin}$ (K)	$\log g$	M ($M_\odot$)	M_V (mag)
				Blue HB stars					
B 577[1]	14.85	−0.04				13 700	3.9	0.45	1.61
B 1509	15.52	−0.06			17 000	17 000	4.1	0.24	2.28
B 2454[1]	14.27	−0.06				10 700	3.5	0.44	1.03
B 4104[1]	15.20	+0.00				17 000	4.0	0.26	1.96
B 4719[1]	15.65	−0.06				16 000	4.0	0.20	2.41
				Stars in the gap region					
B 1628	16.30	−0.17			21 000	21 000	4.7	0.32	3.06
B 2395	16.73	−0.24		21 000	22 000	21 500	5.0	0.43	3.49
B 3655	16.40	−0.22		24 000	22 000	23 000	5.1	0.65	3.16
B 3975	16.27	−0.22		21 000	21 000	21 000	4.8	0.42	3.03
B 4548	16.60	−0.14	22 000	23 000	23 000	22 500	5.2	0.69	3.36
				EHB stars					
B 210	17.04	−0.31			27 000	27 000	5.6	0.82	3.80
B 331[1]	17.12	−0.22				26 000	5.6	0.86	3.88
B 491	17.45	−0.31	28 000	30 000	28 000	28 500	5.3	0.27	4.21
B 617[2]	17.84	−0.33		33 000	26 000	33 000	6.1	0.98	4.60
B 763[1]	17.13	−0.24				27 000	5.5	0.60	3.89
B 916	17.61	−0.26	27 000	30 000	30 000	28 500	5.4	0.29	4.37
B 1288	17.90	−0.31		29 000	27 000	28 000	5.5	0.29	4.66
B 2126	17.28	−0.20		31 000	28 000	29 500	5.7	0.75	4.04
B 2162	17.88	−0.27		35 000	32 000	33 500	5.9	0.57	4.64
B 3915	17.16	−0.23			31 000	31 000	5.5	0.50	3.92
B 4009	17.44	−0.30	33 000	29 000	31 000	31 500	5.7	0.59	4.20
3-118[1]	17.76	−0.26				24 500	5.2	0.20	4.52
				Post-EHB stars					
B 852	15.91	−0.28				39 000	5.2	0.60	2.67
B 1754[1]	15.99	−0.24				40 000	5.0	0.35	2.75
B 4380	15.93	−0.14			32 000	32 000	5.3	0.89	2.69

Notes. [(1)] Data from Heber et al. (1986), adjusted to the Kurucz temperature scale. We note that the mass value for B 1754 given by Cacciari et al. (1995) results from a incorrect bolometric correction (Cacciari, priv. comm.). [(2)] Since B 617 lies close to B 1288 and B 2162 in the CMD we believe that the higher temperature is the correct one (see text [original paper]). It was not taken into account for the mass distribution.

2.10. Moehler et al. (1995, M 15)

See Figs. 11, 12, and Table 10.

The mass values according to Eq. (6) are on average $(12 \pm 11)\%$, $(7.7 \pm 4.6)\%$, $(8.4 \pm 4.3)\%$, $(3.9 \pm 3.7)\%$ lower than the original ones for cases a,b,c, and d in Table 10, respectively. The average mass of the three stars above the gap from the "compromise" method changes from $(0.80 \pm 0.40)\,M_\odot$ to $(0.79 \pm 0.46)\,M_\odot$. All masses shown in Fig. 12 were rederived using the bolometric correction where necessary, that is, for all references except de Boer et al. (1994b).

The average ratio of the derived mass for a given temperature to the theoretically predicted mass on the ZAHB changes from 0.79 to 0.74, which in turn increases the corresponding photometric error from $0\overset{\mathrm{m}}{.}26$ to $0\overset{\mathrm{m}}{.}33$. The conclusions are unaffected by these changes.

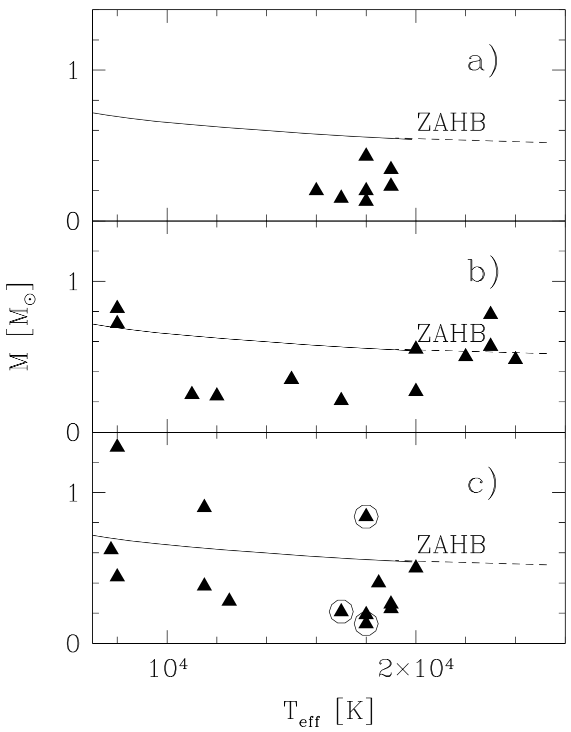

Fig. 11. Figure to replace Fig. 8 in Moehler et al. (1995, M15) The resulting masses for the stars inM15, plotted against $T_{\rm eff}$. The solid line represents a ZAHB model taken from Dorman et al. (1991) for [Fe/H] = −2.26 ($Y_{\rm MS}$ = 0.246, and [O/Fe] = 0.75). The short dashed line represents an extension of the ZAHB towards higher temperatures taken from Sweigart (1987) for $Y_{\rm MS}$0.20 and ZMS = 10^4. *a)* $T_{\rm eff}$ only from low resolution spectra *b)* parameters only from Balmer lines (the masses for B 348 (1.45 $M_\odot$) and B 440 (3.08 $M_\odot$) are left out, because they would corrupt the comparability of the plots) *c)* parameters from combination of continuum (resp. Q index) and Balmer lines. The marked stars are B 208, B 325, and B 276, for which the masses should be treated with great caution (see text [original paper]).

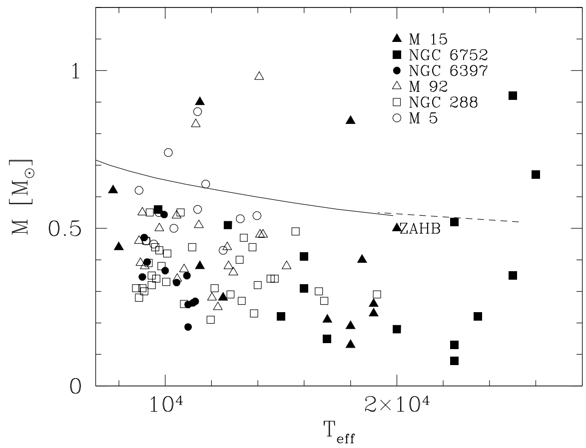

Fig. 12. Figure to replace Fig. 10 in Moehler et al. (1995, M 15). The resulting masses for the stars in M 15 (Table 2c and d [original paper, Table 10 here]), NGC 6752 (Moehler et al. 1994), M 5, M 92, NGC 288 (Crocker et al. 1988), and NGC 6397 (de Boer et al. 1994b) plotted against $T_{\rm eff}$. The solid line represents a ZAHB model taken from Dorman et al. (1991) for [Fe/H] = −2.26 ($Y_{\rm MS}$ = 0.246, and [O/Fe] = 0.75). The short dashed line represents an extension of the ZAHB towards higher temperatures taken from Sweigart (1987) for $Y_{\rm MS}$ = 0.20 and $Z_{\rm MS} = 10^{-4}$.

Table 10. Table to replace Table 2 in Moehler et al. (1995, M 15). Results in M 15. The numbers of the stars refer to Buonanno et al. (1983) and Battistini et al. (1985).

Number	V	$B-V$	M_V	$v_{\rm LSR}$	(a)			(b)			(c)		
					$T_{\rm eff}$	$\log g$	M	$T_{\rm eff}$	$\log g$	M	$T_{\rm eff}$	$\log g$	M
	(mag)	(mag)	(mag)	(km s^{-1})	(K)		($M_\odot$)	(K)		($M_\odot$)	(K)		($M_\odot$)
1	17.85	+0.01	+2.42	−129	18 000	4.10	0.20	22 000	4.70	0.50	19 000	4.30	0.26
20	17.75	−0.02	+2.32	−83	18 000	4.40	0.43	20 000	4.60	0.55	18 500	4.40	0.40
208	18.05	−0.02	+2.62	−95	16 000	4.10	0.20	17 000	4.20	0.21	17 000	4.20	0.21
276	18.52	−0.12	+3.09	−105	18 000	4.20	0.13	24 000	5.00	0.48	18 000	4.20	0.13
421	18.52	−0.03	+3.09	−117	19 000	4.50	0.23	20 000	4.60	0.27	19 000	4.50	0.23
574	17.84	−0.06	+2.41	−102	19 000	4.40	0.34	23 000	4.90	0.78	20 000	4.60	0.50
686	18.42	−0.01	+2.99	−118	17 000	4.20	0.15	23 000	5.00	0.57	18 000	4.30	0.19

Number	V	$B-V$	M_V	$v_{\rm LSR}$	(d)			(b)		
					$T_{\rm eff}$	$\log g$	M	$T_{\rm eff}$	$\log g$	M
	(mag)	(mag)	(mag)	(km s^{-1})	(K)		($M_\odot$)	(K)		($M_\odot$)
18	16.10	+0.11	+0.67	−128	8000	3.50	1.30	8000	3.30	0.82
27	16.66	−0.03	+1.23	−116	12 500	3.50	0.28	12 000	3.40	0.24
258	16.49	+0.06	+1.06	−106	11 500	3.50	0.38	11 000	3.30	0.25
325	16.78	+0.11	+1.35	−126	18 000	4.30	0.84	15 000	3.80	0.35
348	16.69	+0.01	+1.26	−89	11 500	4.00	0.90	12 000	4.20	1.45
440	15.79	+0.22	+0.36	−98	7750	3.00	0.62	7750	3.70	3.08
484	16.04	+0.09	+0.61	−133	8000	3.00	0.44	8000	3.20	0.72

Notes. [(a)] $T_{\rm eff}$ only from continuum; [(b)] parameters only from Balmer lines; [(c)] parameters from combination of continuum and Balmer lines; [(d)] parameters from combination of Q index and Balmer lines.

3. Distances to hot stars in the field

The publications discussed in this section determine effective temperatures and surface gravities of hot subdwarf stars in the field of the Milky Way and derive their distances from the known apparent brightnesses, reddenings, and an assumed mass of 0.5 $M_{\odot}$.

3.1. Theissen et al. (1993)

See Fig. 13 and Tables 11 and 12.

For PG 1701+359 we get a much smaller distance with Eq. (6) than the one listed in Theissen et al. (1993). We think that the original distance is the erroneous one as the theoretical magnitude derived from it differs by $2\overset{\mathrm{m}}{.}5$ from the one corresponding to its atmospheric parameters. Excluding this object the distance values according to Eq. (9) are on average (3.8 ± 6.2)% larger than the original ones. With the new distances we derive a slightly lower scale height of 170^{+100}_{-40} pc, whose smaller error bares are probably due to the improved distance for PG 1701+359. With the new scale height the derived space density changes from $1.9^{+3.24}_{-1.34} \times 10^{-6}$ pc^{-3} to $2.2^{+1.9}_{-1.3} \times 10^{-6}$ pc^{-3}. The conclusions are not affected.

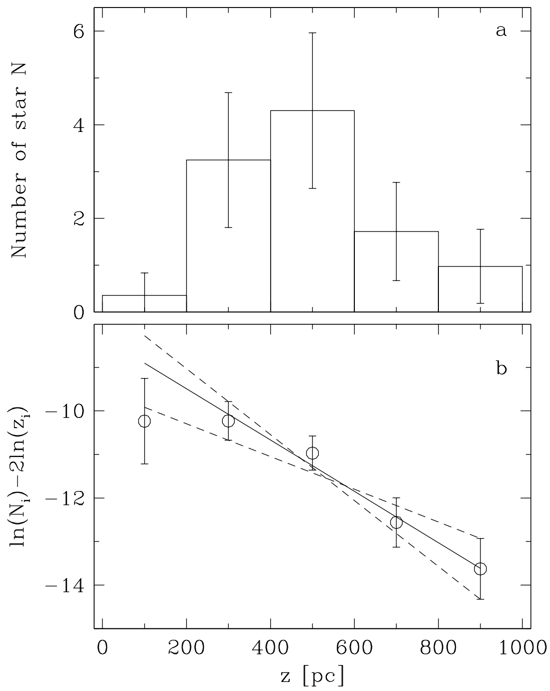

Fig. 13. Figure to replace Fig. 6a and b in Theissen et al. (1993). *a)* Average distribution of the statistically complete sample perpendicular to the galactic plane, created by 10 000 Monte Carlo simulations. *b)* Regression of $\ln N_i - 2 \ln z_i$ to determine the scale height which follows from the negative inverse of the slope. N_i denotes the number of stars in bin i, z_i the distance. The full drawn line is the least square fit, weighted with the inverse errors; the dashed lines are extreme fits giving the errors in scale height.

Table 11. Table to replace Table 3 of Theissen et al. (1993). Atmospheric parameters, interstellar extinctions, and distances of the single stars.

Object	$T_{\rm eff}$ (K)	$\log g$ (cm s^{-2})	A_y (mag)	r (pc)	z (pc)
PG 1656+318	29 900 ± 800	5.25	0.098	1430	860
PG 1708+602	35 900 ± 1900	5.0	−0.092	1700	1000
PG 1710+490	28 600 ± 3000	5.45	0.085	630	370
PG 1716+426*	25 600 ± 900	5.2	0.043	1300	730
PG 1722+286	31 700 ± 1700	5.4	−0.047	880	450
PG 1725+252	26 000 ± 400	5.25	0.166	710	340
PG 1738+505	24 700 ± 700	5.05	0.009	1030	540
PG 1739+489	24 400 ± 700	5.15	0.043	880	460
PG 1743+477*	27 400 ± 2000	5.45	0.111	930	480
PG 2059+013	26 300 ± 1200	5.05	0.047	2500	1170

Notes. (*) Also described in Paper II (Moehler et al. 1990).

Table 12. Table to replace Table 4 of Theissen et al. (1993). Deconvolved photometry, atmospheric parameters, and distances of the binary stars.

Object	y (mag)	$b-y$ (mag)	$u-b$ (mag)	$c1$ (mag)	$T_{\rm eff}$ (K)	$\log g$ (cm s^{-2})	r (pc)	z (pc)	A_y (mag)
PG1647+253	14.179(095)	−0.131(40)	−0.272(47)	−0.251(30)	36 500 ± 1500	6.00	690	420	0.144
PG1701+359	13.250(089)	−0.124(29)	−0.095(44)	−0.123(28)	26 250 ± 1250	5.80	480	290	0.048
PG1718+519	14.284(019):	−0.087(23):	+0.037(10):	−0.294(10):	23 500 ± 1000:	4.25:	4120:	2370:	0.048
PG2110+127	13.230(011):	−0.082(10):	−0.045(06):	−0.297(04):	25 400 ± 1600:	4.20:	2670:	1070:	0.240
PG2259+134	14.635(146)	−0.118(42)	−0.138(79)	−0.154(55)	28 500 ± 1600	5.30	1650	1090	0.144
PG2331+038*	15.090(150)	−0.114(42)	−0.102(80)	−0.063(53)	27 200 ± 1500	5.30	1940	1570	0.144
PG2337+070*	13.613(132)	−0.112(41)	−0.090(67)	−0.064(40)	27 250 ± 1350	5.30	950	750	0.240
PHL1079*	13.601(167)	−0.110(43)	−0.085(73)	−0.217(60)	26 350 ± 1450	5.10	1270	1070	0.048

Notes. (*) Also discussed in Paper II (Moehler et al. 1990).

3.2. Moehler et al. (1990)

See Figs. 14, 15, and Table 13.

The distance values according to Eq. (9) are on average $(6.8 \pm 2.5)\%$ larger than the original ones. The scale height changes from (250 ± 45) pc to (230 ± 30) pc and the space density changes from 1×10^{-6} pc^{-3} to 1.1×10^{-6} pc^{-3}. The conclusions are not affected.

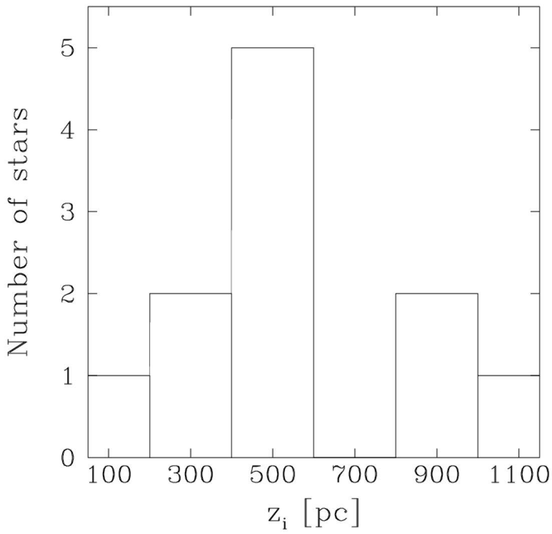

Fig. 14. Figure to replace Fig. 5 in Moehler et al. (1990). z distribution histogram of the sdB stars in the statistical-complete part of our sample.

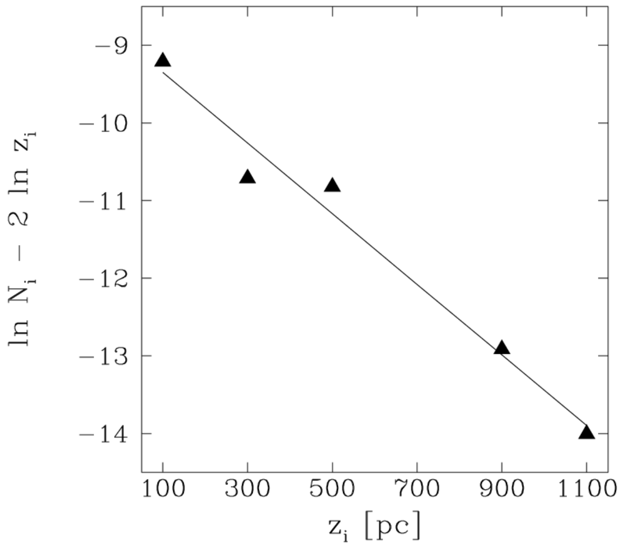

Fig. 15. Figure to replace Fig. 6 in Moehler et al. (1990). Determination of the scale height z_s from the regression of $\ln N_i - 2 \ln z_i$. The full drawn line gives the regression resulting from the stars of our statistically complete sample.

Table 13. Table to replace Table 4 of Moehler et al. (1990). Physical parameters derived for the programme sdB stars.

Object	$T_{\rm eff}$ (K)	$\log g$ (cm s^{-2})	V or y (mag)	A_V or A_y (mag)	d (pc)	l (deg)	b (deg)	z (pc)
PG 0004+133	24 700	4.5	13.060	0.482	1500 ± 580	106.9	−47.9	1120 ± 430
PG 0039+049	26 700	4.7	12.889	0.629	1100 ± 420	118.6	−57.6	940 ± 350
PG 0101+039[a]	25 700	5.3	12.070	0.038	500 ± 190	129.1	−58.5	430 ± 160
PG 0133+114	26 400	4.9	12.280	0.152	840 ± 320	140.1	−49.7	640 ± 240
PHL 1079	32 000	5.5	13.38	0.593	650 ± 240	144.9	−57.1	540 ± 200
PG 0142+148	26 200	5.1	13.726	0.146	1310 ± 500	141.9	−45.8	940 ± 360
PG 0209−015	23 500	4.9	14.047	0.000	1790 ± 680	162.9	−57.7	1510 ± 580
PG 0212+148	25 000	5.0	14.482	0.226	1890 ± 760	151.2	−43.2	1300 ± 520
PG 0212+143	25 400	5.0	14.584	0.226	1990 ± 780	151.7	−43.6	1380 ± 540
PG 0242+132	26 500	4.7	13.220	0.341	1500 ± 560	160.9	−40.9	980 ± 370
PG 0342+026[b]	24 000	4.9	10.944	0.324	380 ± 140	184.4	−38.5	230 ± 90
PG 0856+121	23 800	5.1	13.473	0.094	1050 ± 390	216.5	+33.7	580 ± 330
PG 0907+123	26 300	5.0	13.937	0.094	1620 ± 610	217.7	+36.3	960 ± 360
PG 0918+029	29 300	5.2	13.319	0.000	1080 ± 420	229.4	+34.3	610 ± 230
PG 1255+544	31 300	5.5	13.533	0.040	890 ± 330	120.9	+62.7	790 ± 300
PG 1303−114	28 500	5.1	13.959	−0.081∗	1630 ± 610	308.7	+51.0	1260 ± 480
PG 1432+004	22 400	5.0	12.759	0.105	810 ± 310	350.1	+53.3	650 ± 250
PG 1452+198	26 400	5.0	12.476	−0.035∗	880 ± 320	24.7	+60.8	760 ± 280
PG 1458+423	28 000	5.3	13.79	0.058	1140 ± 430	71.0	+59.8	580 ± 220
PG 1519+640	27 000	5.2	12.458	−0.047∗	690 ± 250	100.3	+46.2	500 ± 190
PG 1532+523	29 800	5.4	14.043	−0.037∗	1240 ± 460	83.8	+50.8	960 ± 360
PG 1559+533	26 300	5.2	14.392	−0.193∗	1660 ± 610	83.0	+46.5	1200 ± 460
PG 1613+467	25 000	5.3	14.58	−0.102∗	1560 ± 590	73.0	+45.8	1110 ± 420
PG 1619+522	31 000	5.5	13.297	0.004	790 ± 300	80.5	+44.0	550 ± 210
PG 1644+403	31 000	5.6	15.40	0.179	1720 ± 650	64.1	+40.4	1110 ± 420
PG 1645+610	26 200	5.3	14.507	0.343	1360 ± 520	90.9	+38.6	850 ± 320
PG 1648+536	30 100	5.3	14.055	0.180	1300 ± 490	81.4	+39.4	830 ± 310
PG 1656+600	25 000	5.3	15.82	0.000	2750 ± 1030	89.3	+37.5	1680 ± 630
PG 1710+490	28 300	5.3	12.900	0.075	770 ± 290	75.4	+36.1	450 ± 170
PG 1716+426	25 200	5.3	13.967	−0.002∗	1170 ± 440	67.7	+34.6	660 ± 250
PG 1743+477	25 900	5.5	13.787	0.088	840 ± 310	74.4	+30.7	430 ± 160
PG 2204+035	29 800	5.4	14.245	0.200	1240 ± 470	64.4	−39.8	800 ± 310
PG 2314+076	25 700	5.1	13.758	0.238	1250 ± 480	86.5	−48.3	940 ± 350
PG 2331+038	26 900	5.5	14.929	0.384	1290 ± 490	89.1	−53.6	1040 ± 390
PG 2337+070	27 000	5.2	13.47	0.486	880 ± 330	93.8	−51.4	690 ± 250
PG 2349+002	24 700	5.2	13.268	0.149	860 ± 340	93.1	−58.9	740 ± 290
PG 2358+107	25 500	5.3	13.624	0.260	900 ± 340	103.5	−50.0	690 ± 260

Notes. [(a)] Heber & Langhans (1986) derived $T_{\rm eff}$ = 26 900 K , $\log g$ = 5.5, and A_V = 0.016. [(b)] Lamontagne et al. (1987) derived $T_{\rm eff}$ = 21 800 K, $\log g$ = 5.0, and A_V = 0.192. [(∗)] A negative extinction resulted from colour $(b - y)$ respectively $(B - V)$ that were bluer than predicted from the model atmospheres. For the determinations of the stars' distance they were set equal to 0.000.

4. Publications using distances for further analysis

In this section we describe – where known – the effects of the erroneous distances on further analyses. The information for de Boer et al. (1994a); Colin et al. (1994); Centurión et al. (1994); de Boer et al. (1997); Geffert (1998); Altmann et al. (2004) and Smoker et al. (2004, 2006) were kindly provided by K. S. de Boer and J. V. Smoker, respectively.

4.1. de Boer et al. (1994, distances to high-velocity clouds)

For the determination of the lower limit to the distance of the high-velocity gas Complex C three stars from Moehler et al. (1990) were used. The distance of these stars ought to have been on average (4.8 ± 1.6)% larger, but this is an insignificant change in relation with the other uncertainties for such a determination. This publication was ultimately superseded by the review by van Woerden & Wakker (2004).

4.2. Colin et al. (1994, kinematics of sdB stars)

This first paper on galactic orbits of sdB stars used six stars from the Moehler et al. (1990) paper. Distances were on average (7 ± 6)% too small. The conclusions are unaffected and this research was much extended by de Boer et al. (1997), using 41 stars.

4.3. Centurión et al. (1994, distances to high-velocity gas)

Using the presence or absence of Na I and Ca II interstellar absorption lines towards various stars from Moehler et al. (1990) and Theissen et al. (1993), distance limits for high-velocity gas clouds were attempted to be obtained. Correcting for the revised distances as given in the above sections leads to the following results. Towards Complex C I the stellar distance now is 6% larger and the distance to the gas becomes larger accordingly. Towards Complex C IB the distance to the three stars used are on average 1% larger, so a negligible effect on the conclusions. Towards the Magellanic Stream, the three stars used are on average 7% more distant, but the conclusions are unchanged. Towards the Anticentre Cohen Stream the stellar distances are on average unchanged, so the conclusions are unaffected. Towards the AC complexes the stellar distances are now 7% larger but no interstellar absorption lines had been detected.

4.4. de Boer et al. (1997, kinematics of sdB stars)

The distribution perpendicular to the galactic plane of sdB stars was derived from sdB star orbits. 22 of the 41 stars came from Moehler et al. (1990). The paper also contains a discussion of the effects errors in the distances would have. A subset of the astrometric sample had been taken from Saffer et al. (1994) whose distances were smaller by up to a factor of 1.5 than distances derived with our methods. Due to the script error, the distances of the 22 Moehler et al. (1990) sdB stars included in the orbit study have to be to corrected upwards by on average 6.3%. This would increase the derived scale height by a few percent. That change is well within all other uncertainty limits so the conclusion of the paper, including the value of the scale height, stays unchanged.

4.5. Geffert (1998, kinematics)

Using Hipparcos data for fields around the globular clusters M 3 and M 92, also for the star PG 1716+426 the proper motion could be derived. The orbit calculated used the distance from Theissen et al. (1993) of 1200 ± 300 pc. The revised distance is 1300 ± 330 pc (see Table 12 above), well inside the margin of uncertainty, and this small change does not affect the conclusions of the paper.

4.6. Heber et al. (2002, resolving binary sdB stars)

This paper used WFPC2 images from the *Hubble* Space Telescope to resolve subdwarf B star systems that showed indications for late-type companions. The change of distance for PG 1718+519 from 810 pc to 880 pc changes the linear separation of the two components for that system from 230 AU to 240 AU. The conclusions are unaffected.

4.7. Altmann et al. (2004, kinematics of sdB stars)

This study considerably extended the above mentioned work by de Boer et al. (1997), now including 114 stars. The orbits and the overall spatial distribution of the sdB stars are based on distances derived with a different method than the one from Moehler et al. (1990). However, 19 stars from de Boer et al. (1997) were included, among them 17 with distances from the script used by Moehler et al. (1990). Again, distances of these 17 stars ought to have been larger by on average 6.3%. Since these stars form only a small fraction of the sample, the conclusions of this paper remain unchanged.

4.8. Smoker et al. (2004, 2006, distances to intermediate- and high-velocity clouds)

These publications used spectra of early-type stars to determine distances to intermediate- and high-velocity clouds and Ca abundances of the low velocity gas in front of these clouds. They used (among others) the stars PG 1710+426 (Moehler et al. 1990), PG 1718+519, PG 1725+252, PG 1738+505, and PG 1739+489 (all from Theissen et al. 1993), whose distances according to Eq. (9) are on average (6.8 ± 1.6)% larger than the original ones. This does not affect their conclusions.

Acknowledgements. We thank K. S. de Boer for his help with evaluating the impact on publications using the original distances. This research has made use of NASA's Astrophysics Data System Bibliographic Services.

References

Altmann, M., Edelmann, H., & de Boer, K. S. 2004, A&A, 414, 181

Battistini, P., Bregoli, G., Fusi Pecci, F., Lolli, M., & Epps Bingham, E. A. 1985, A&AS, 61, 487

Buonanno, R., Buscema, G., Corsi, C. E., Iannicola, G., & Fusi Pecci, F. 1983, A&AS, 51, 83

Buonanno, R., Caloi, V., Castellani, V., et al. 1986, A&AS, 66, 79

Cacciari, C., Fusi Pecci, F., Bragaglia, A., & Buzzoni, A. 1995, A&A, 301, 684

Caloi, V., Castellani, V., Danziger, J., et al. 1986, MNRAS, 222, 55

Centurión, M., Vladilo, G., de Boer, K. S., Herbstmeier, U., & Schwarz, U. J. 1994, A&A, 292, 261

Colin, J., de Boer, K. S., Dauphole, B., et al. 1994, A&A, 287, 38

Crocker, D. A., Rood, R. T., & O'Connell, R. W. 1988, ApJ, 332, 236

de Boer, K. S., Altan, A. Z., Bomans, D. J., et al. 1994a, A&A, 286, 925

de Boer, K. S., Schmidt, J. H., & Heber, U. 1994b, in Proc. Hot Stars in the Galactic Halo, eds. S. J. Adelman, A. R. Upgren, & C. J. Adelman (CUP), 277

de Boer, K. S., Schmidt, J. H. K., & Heber, U. 1995, A&A, 303, 95

de Boer, K. S., Aguilar Sanchez, Y., Altmann, M., et al. 1997, A&A, 327, 577

Dorman, B., Lee, Y.-W., & Vandenberg, D. A. 1991, ApJ, 366, 115
Dorman, B., Rood, R. T., & O'Connell, R. W. 1993, ApJ, 419, 596
Dreizler, S., Heber, U., Werner, K., Moehler, S., & de Boer, K. S. 1990, A&A, 235, 234
Flower, P. J. 1996, ApJ, 469, 355
Geffert, M. 1998, A&A, 340, 305
Harris, W. E. 1996, AJ, 112, 1487
Heber, U., & Langhans, G. 1986, in New Insights in Astrophysics, Eight Years of UV Astronomy with IUE, ed. E. J. Rolfe, ESA SP, 263, 279
Heber, U., Kudritzki, R. P., Caloi, V., Castellani, V., & Danziger, J. 1986, A&A, 162, 171
Heber, U., Moehler, S., Napiwotzki, R., Thejll, P., & Green, E. M. 2002, A&A, 383, 938
Kurucz, R. L. 1992, in The Stellar Populations of Galaxies, eds. B. Barbuy, & A. Renzini, IAU Symp., 149, 225
Lamontagne, R., Wesemael, F., & Fontaine, G. 1987, ApJ, 318, 844
Moehler, S., & Sweigart, A. V. 2006, A&A, 455, 943
Moehler, S., de Boer, K. S., & Heber, U. 1990, A&A, 239, 265
Moehler, S., Heber, U., & de Boer, K. S. 1994, in Proc. Hot Stars in the Galactic Halo, eds. S. J. Adelman, A. R. Upgren, & C. J. Adelman (CUP), 217
Moehler, S., Heber, U., & de Boer, K. S. 1995, A&A, 294, 65
Moehler, S., Heber, U., & Rupprecht, G. 1997, A&A, 319, 109
Moehler, S., Landsman, W., & Napiwotzki, R. 1998, A&A, 335, 510
Moehler, S., Landsman, W. B., & Dorman, B. 2000a, A&A, 361, 937
Moehler, S., Sweigart, A. V., Landsman, W. B., & Heber, U. 2000b, A&A, 360, 120
Moehler, S., Landsman, W. B., Sweigart, A. V., & Grundahl, F. 2003, A&A, 405, 135
Moehler, S., Dreizler, S., Lanz, T., et al. 2011, A&A, 526, A136
Moehler, S., Dreizler, S., LeBlanc, F., et al. 2014, A&A, 565, A100
Moni Bidin, C., Moehler, S., Piotto, G., Momany, Y., & Recio-Blanco, A. 2007, A&A, 474, 505
Moni Bidin, C., Moehler, S., Piotto, G., Momany, Y., & Recio-Blanco, A. 2009, A&A, 498, 737
Moni Bidin, C., Villanova, S., Piotto, G., Moehler, S., & D'Antona, F. 2011, ApJ, 738, L10
Saffer, R. A., Bergeron, P., Koester, D., & Liebert, J. 1994, ApJ, 432, 351
Salgado, C., Moni Bidin, C., Villanova, S., Geisler, D., & Catelan, M. 2013, A&A, 559, A101
Smoker, J. V., Lynn, B. B., Rolleston, W. R. J., et al. 2004, MNRAS, 352, 1279
Smoker, J. V., Lynn, B. B., Christian, D. J., & Keenan, F. P. 2006, MNRAS, 370, 151
Sweigart, A. V. 1987, ApJS, 65, 95
Theissen, A., Moehler, S., Heber, U., & de Boer, K. S. 1993, A&A, 273, 524
van Woerden, H., & Wakker, B. P. 2004, in High Velocity Clouds, eds. H. van Woerden, B. P. Wakker, U. J. Schwarz, & K. S. de Boer, Astrophys. Space Sci. Lib., 312, 195